

22. Wainscoat, R. J. & Cowie, L. L. A filter for deep near-infrared imaging. *Astron. J.* 103, 332–337 (1992).
 23. Stetson, P. B. DAOPHOT: a computer program for crowded-field stellar photometry. *Publ. Astron. Soc. Pacif.* 99, 191–222 (1987).

Acknowledgements. We thank B. Schaeffer and W. Harrison for their assistance at the telescope. Data presented here were obtained at the W.M. Keck Observatory, which is operated as a scientific partnership between the California Institute of Technology, the University of California, and NASA. The Observatory was made possible by the generous financial support of the W.M. Keck Foundation. This work was performed in part at the Jet Propulsion Laboratory, California Institute of Technology, under a contract with NASA.

Correspondence and requests for materials should be addressed to E.S. (e-mail: serabyn@tacos.caltech.edu).

Self-organized growth of nanostructure arrays on strain-relief patterns

Harald Brune, Marcella Giovannini, Karsten Bromann & Klaus Kern

Institut de Physique Expérimentale, EPF Lausanne, CH-1015 Lausanne, Switzerland

The physical and chemical properties of low-dimensional structures depend on their size and shape, and can be very different from those of bulk matter. If such structures have at least one dimension small enough that quantum-mechanical effects prevail, their behaviour can be particularly interesting. In this way, for example, magnetic nanostructures can be made from materials that are non-magnetic in bulk¹, catalytic activity can emerge from traditionally inert elements such as gold², and electronic behaviour useful for device technology can be developed^{3,4}. The controlled fabrication of ordered metal and semiconductor nanostructures at surfaces remains, however, a difficult challenge. Here we describe the fabrication of highly ordered, two-dimensional nanostructure arrays through nucleation of deposited metal atoms on substrates with periodic patterns defined by dislocations that form to relieve strain. The strain-relief patterns are created spontaneously when a monolayer or two of one material is deposited on a substrate with a different lattice constant. Dis-

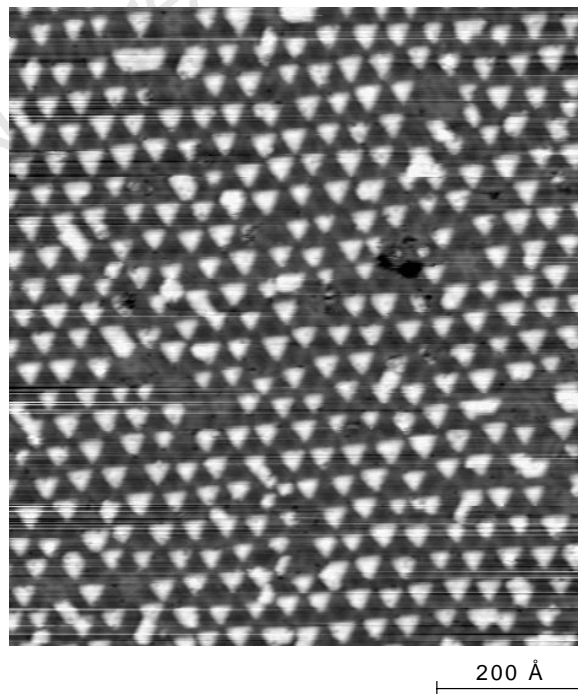


Figure 1 STM image of a periodic array of Fe islands nucleated on the dislocation network of a Cu bilayer on Pt(111) at 250 K.

locations often repel adsorbed atoms diffusing over the surface, and so they can serve as templates for the confined nucleation of nanostructures from adatoms. We use this technique to prepare ordered arrays of silver and iron nanostructures on metal substrates.

Arbitrary atomic-scale structures can be assembled with the tip of a scanning tunnelling microscope (STM), either through direct displacement of adsorbed atoms⁵, or through tip-assisted decomposition of chemical species⁶. The principal drawback of methods based on scanning probes is their serial character. Approaches where a large number of structures can be created in parallel are self-organized growth—either in the kinetic⁷ or in the thermodynamic regime^{8–10}—and the controlled deposition of size-selected clusters from the gas phase¹¹. Whereas the latter technique produces nanostructures of nearly uniform sizes on surfaces, the self-organized growth suffers from broad size distributions. In addition, both methods yield largely uncorrelated spatial distributions caused by the statistics of deposition and diffusion.

There have been several attempts to improve the spatial order in nanostructure growth. The vertical correlation of island nucleation in sequences of quantum dot and spacer layers yielded improved lateral order¹². Also, misfit dislocations have been used for nanoscale structuring. Preferred nucleation of Ni at dislocations of the Au(111) reconstruction resulted in ordered islands¹³; for this system, the mechanism was identified as site-specific exchange, a finding that strongly reduces the number of elements suitable for this type of ordering¹⁴. Also in semiconductors, island accumulation at dislocations has been reported¹⁵. However, there the bulk-like dislocations were not mobile enough to order into periodic patterns. Due to the attraction towards dislocations, islands were lined up in one dimension but were not periodic in two dimensions.

In heteroepitaxial systems that show strain relief through dislocations, the dislocations quite often arrange into highly ordered periodic patterns. This is due to mutual long-range repulsion and

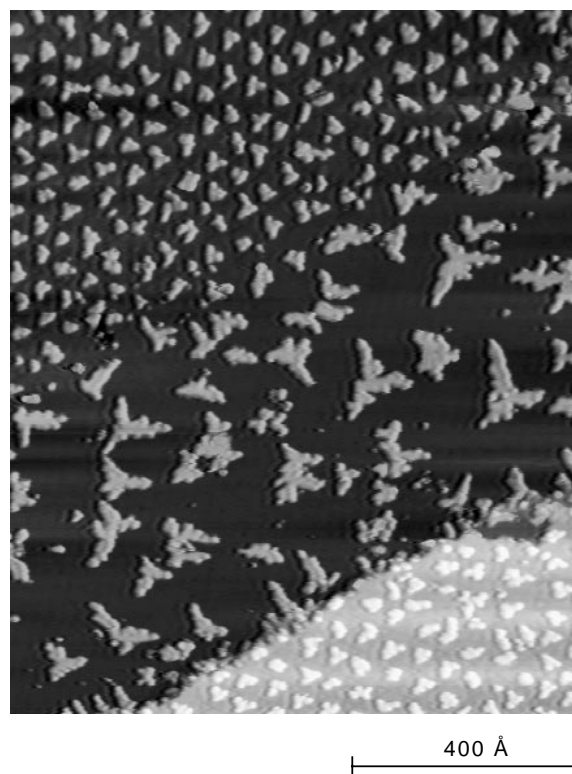


Figure 2 STM image of periodically ordered versus randomly nucleated islands on a heterogeneous substrate. The islands were grown by deposition of 0.1 ML Ag at 110 K onto a Pt(111) surface pre-covered by 1.5 ML Ag (1 ML is one adsorbed atom per substrate atom).

high mobility of the dislocations located at the surface. These surface dislocations are often strongly repulsive towards diffusing adatoms. Here we show that this can be used to transfer the dislocation periodicity through heterogeneous nucleation to regular superlattices of almost mono-dispersed islands. We demonstrate the feasibility of this self-organized growth method with Fe islands on the second monolayer (ML) of Cu on a Pt(111) substrate (Fig. 1), and with Ag nucleation on 2 ML of Ag on Pt(111) (Figs 2 and 3). The array of Fe quantum dots in Fig. 1 shows the unique potential of the approach. The areal density of the Fe dots exceeds the densities at present achieved by electron-beam lithography by two orders of magnitude.

Random versus ordered nucleation are contrasted in the STM image shown in Fig. 2. Quite regularly spaced islands coexist with a part of the surface covered by randomly distributed islands. While the latter show the broad distribution of island size (Fig. 3c) and distance typically observed for nucleation on isotropic substrates, the former appear to be placed on a periodic grid. This marked difference is caused by the structure of the underlying substrate. Before growing the Ag islands, the Pt(111) substrate was pre-

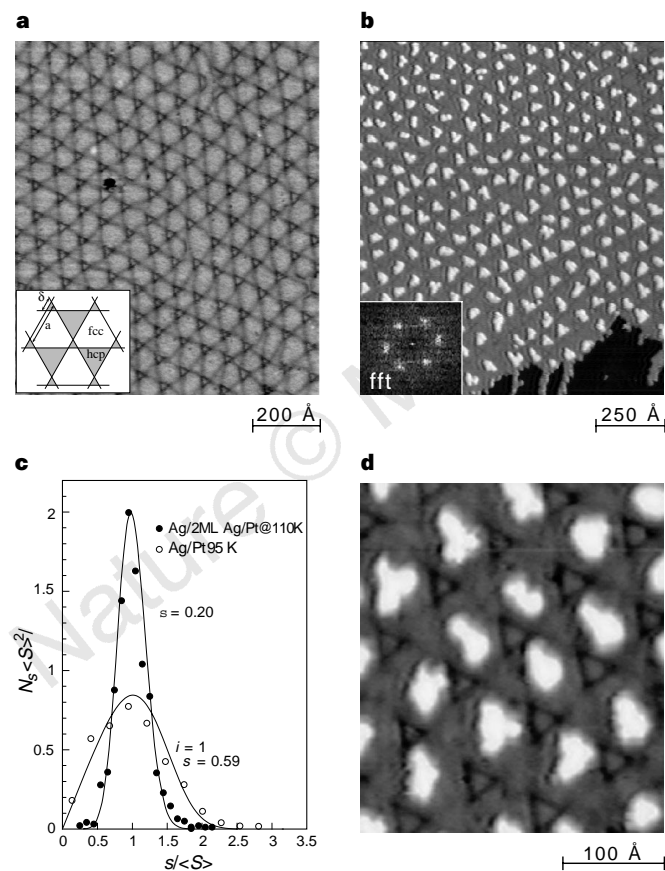


Figure 3 STM images showing the confined nucleation of adatom islands on a dislocation network. **a**, STM image of the ordered (25 × 25) dislocation network formed by the second Ag monolayer on Pt(111) on deposition at 400K and subsequent annealing to 800K. The inset shows a model of this trigonal strain-relief pattern. **b**, A superlattice of islands is formed on Ag deposition onto this network at 110K (coverage $\theta = 0.10$ ML). Inset, the Fourier transform of the STM image shows the high degree of order and the hexagonal symmetry of the nanostructure array. **c**, Island size distributions for random and ordered nucleation (curves, theory; dots, experiment). The curve for ordered nucleation is a binomial fit. The curve labelled $i = 1$ shows the size distribution from scaling theory for random nucleation on an isotropic substrate. Size distributions were normalized according to scaling theory (s is the island size in atoms, $\langle S \rangle$ its mean value, and $N_s \langle S \rangle^{-2}$ the density of islands with size s per substrate atom). **d**, Detail of STM image **b**.

covered by 1.5 ML Ag such that the first and second monolayer coexist. These two layers differ in structure. The lattice constant of Ag is 4.3% larger than that of Pt. In the first monolayer, the Ag atoms are coherently strained by this amount and form a pseudomorphic layer¹⁶. As this layer is homogeneous (and isotropic), one observes random nucleation on top of it.

The second monolayer of Ag, on the other hand, forms a trigonal network of dislocations in which the compressive strain is partially relieved¹⁷. This network reveals a well established long-range order (Fig. 3a). The dislocations mark transitions from face-centred cubic (f.c.c.) to hexagonal close-packed (h.c.p.) stacking. Larger areas with the energetically favoured f.c.c. stacking are achieved by displacing one class of domain walls (Fig. 3a inset) relative to the crossing point of the two others. The resulting unit cell has trigonal symmetry and consists of a large quasi-hexagon (f.c.c.) and two triangles with opposite orientation (h.c.p. stacking).

Nucleation of Ag onto this network at low temperature leads to a high density of islands (Fig. 4), most of which are located away from dislocations. This implies that dislocations are repulsive barriers towards diffusing adatoms. At $T = 110$ K, the island density approaches a stationary value of exactly one island per network unit cell (Fig. 3b). We note that all islands nucleate within the distorted hexagons (Fig. 3d). This implies preferential binding to f.c.c.-areas in agreement with theory¹⁸. Owing to this difference in binding energy, atoms landing on h.c.p. triangles can diffuse into the f.c.c. hexagons but not vice versa. The repulsive nature of the dislocations and the attraction towards specific sites within the unit cell are the key properties transferring the periodicity of the dislocation network to a highly ordered two-dimensional island superlattice.

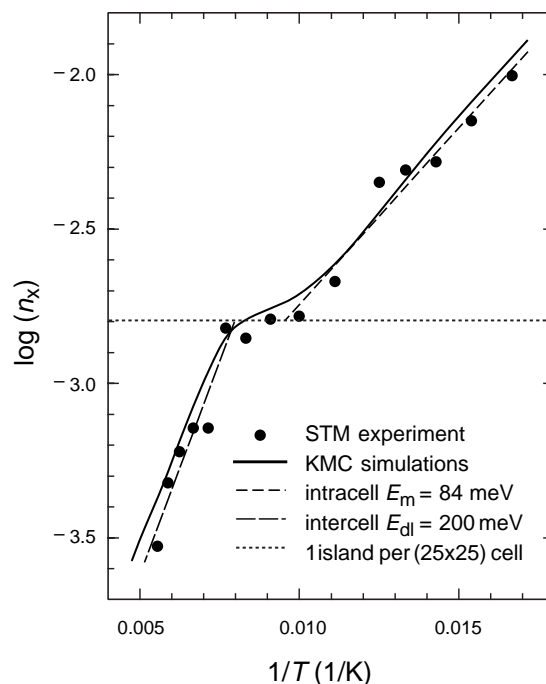


Figure 4 Arrhenius plot of measured (dots) and simulated (curve) island densities, n_x , for nucleation of 0.1 ML Ag on the dislocation network of Fig. 3a. The experimental island densities clearly show two slopes separated by a plateau with a density of one island per superstructure unit cell. The plateau is less pronounced in the Monte Carlo simulations than in the experiment. In the experiment, dislocations have a long-range repulsion towards adatoms, funneling them to the unit-cell centre where the islands are nucleating. We did not attempt to simulate the complicated energy surface required to account for these findings. The islands in the simulation are therefore randomly placed within the unit cells; those located at the border sometimes overgrow a dislocation which smears out the plateau.

